

Article

# Thermal Properties of PEG/Graphene Nanoplatelets (GNPs) Composite Phase Change Materials with Enhanced Thermal Conductivity and Photo-Thermal Performance

Lihong He <sup>1,2,\*</sup>, Hao Wang <sup>1,2,\*</sup>, Hongzhou Zhu <sup>2</sup>, Yu Gu <sup>3</sup>, Xiaoyan Li <sup>1</sup> and Xinbo Mao <sup>1</sup>

<sup>1</sup> School of Materials Science and Engineering, Chongqing Jiaotong University, Chongqing 400074, China; 990201400027@cqjtu.edu.cn (X.L.); maixinbo\_19930303@163.com (X.M.)

<sup>2</sup> The National Joint Engineering Laboratories of Traffic Civil Materials, Chongqing Jiaotong University, Chongqing 400074, China; zhuhongzhouchina@126.com

<sup>3</sup> The Key Laboratory of Road and Traffic Engineering, Ministry of Education, Tongji University, No. 4800 Cao'an Road, Shanghai 201804, China; guyu8241183@163.com

\* Correspondence: sunnyhlh@126.com (L.H.); SodaWangHao@163.com (H.W.); Tel.: +86-138-9602-3469 (L.H.); +86-132-0616-7705 (H.W.)

Received: 3 November 2018; Accepted: 9 December 2018; Published: 13 December 2018



**Abstract:** This paper mainly concentrates on the thermal conductivity and photo-thermal conversion performance of polyethylene glycol (PEG)/graphene nanoplatelets (GNPs) composite phase change materials (PCMs). The temperature-assisted solution blending method is used to prepare PCM with different mass fraction of GNPs. According to the scanning electron microscope (SEM), GNPs are evenly distributed in the PEG matrix, forming a thermal conduction pathway. The Fourier transform infrared spectra (FT-IR) and X-ray diffraction (XRD) results show that the composites can still inherit the crystallization structure of PEG, moreover, there are only physical reactions between PEG and GNPs rather than chemical reactions. Differential scanning calorimeter (DSC) and thermal conductivity analysis results indicate that it may be beneficial to add a low loading ration of GNPs to obtain the suitable latent heat as well as enhance the thermal conductivity of composites. To investigate the change in the rheological behavior due to the effect of GNPs, the viscosity of the composites was measured as well. The photo-thermal energy conversion experiment indicates that the PEG/GNPs composites show better performance in photothermal energy conversion, moreover, the Ultraviolet-visible-Near Infrared spectroscopy is applied to illustrate the reasons for the higher absorption efficiency of PEG/GNPs for solar irradiation.

**Keywords:** polyethylene glycol; phase change materials; graphene nanoplates; thermal conductivity; photo-thermal conversion performance

## 1. Introduction

The rapid consumption of fossil fuels and the increasing contradiction between energy supply and demand are compelling researchers to utilize energy more effectively and develop renewable energy [1]. A solar energy source, which is inexhaustible, economical and environmentally friendly, has been widely recognized as an ideal form of renewable energy [2]. In recent years, the conversion of photo-thermal technology is the most successful and popular technique among the different forms of solar energy utilization, such as light-thermal conversion, light-electricity conversion, light-biology conversion [3]. Photo-thermal applications not only possess the merits of relatively high photo-thermal energy conversion efficiency but also can be achieved without complicated

and expensive instruments [4,5]. However, there are still some nonnegligible drawbacks in the use of solar energy, such as low conversion efficiency, diurnal fluctuation of optical radiation, which limit the efficient utilization of solar thermal energy storage [4]. Latent heat thermal energy storage (LHTES) system has proved to be a promising technique for overcoming the drawbacks of solar energy conservation because of its outstanding advantages, such as high heat storage density, constant operating temperature, isothermal characteristics. In recent years, LHTES has been widely applied to various thermal storage management applications [6–9]. Phase change materials (PCMs), as representative of advanced LHTES materials, are the most prevalent and effective technique for thermal energy storage because of their high enthalpy change, non-toxic, and reusability characteristic, which can be utilized in a range of applications, such as thermal management of solar energy, insulation clothing, thermal insulation buildings, spacecraft thermal control and so on [10–14].

Among various organic PCMs (OPCMs), polyethylene glycol (PEG) is universally recognized as a kind of outstanding solid-liquid transformation PCM because of its excellent properties, including economically available, high phase change enthalpy, biodegradation, little subcooling, low vapor pressure, non-toxicity [14–16]. In addition, it is convenient to obtain the suitable phase change temperature and enthalpy via simply changing molecular weight of PEG [17]. However, the pristine PEG as OPCMs in the utilization of solar energy has intrinsic shortcomings, including low thermal conductivity and poor absorptive performance in the optical light, which accounts for 50% of the solar radiation energy. The former refers to the speed of absorbing and releasing thermal energy, which can reduce the energy efficiency [18]. The latter leads to low solar energy efficiency, which limits its applications of solar thermal energy to a great extent. Consequently, the thermal conductivity and photothermal performance of OPCM are imperative to be enhanced.

Hence, many prominent works have been done to obtain the PCMs with much higher thermal conductivity. A prevalent approach against this shortcoming is to incorporate the highly thermal conductive fillers into the PCMs, such as silver nanowire [19], Cu [20], TiO<sub>2</sub> nanoparticles [21]. Deng et al. [19] achieved PEG-Ag/expanded vermiculite PCMs by the physical blending and impregnation method. The thermal conductivity increased to 0.68 W/(mK) for 19.3 wt % silver nanowire in the composite PCMs, which was 11.3 times higher than that of pristine PEG. Zhang et al. [20] prepared composite PCMs by adding Cu powder to PEG/SiO<sub>2</sub> through the sol-gel method, and discovered that the thermal conductivity of the composite PCMs reached up to 0.431 W/(mK) by an addition of 3.45 wt % Cu powder, which was enhanced by 49.13% in comparison with pure PEG. Harikrishnan et al. [21] used a two-step method to prepare stearic acid-TiO<sub>2</sub> nanofluids PCMs. For composite with only 0.3 wt % TiO<sub>2</sub>, the enhancement of thermal conductivity was measured to be 70.52%. However, the aforementioned composite PCMs are white powders, which present poor absorptive performance in the optical light, resulting in a weak photothermal conversion property and a low solar energy utilization ratio. Therefore, the carbon materials are good additives for improving the optical absorption performance of PCMs because of their high visible light absorptivity. Graphene nanoplates (GNPs) are thin flat particles that consist of single and few layer graphene mixed with thicker graphite, thus, structurally they are in between graphene and graphite [22]. Compared to other carbon-based materials, GNPs possess many outstanding functional performance, such as unique photonic/optical transportation, light weight, high thermal/electrical conductivity, excellent mechanical property [23,24]. Furthermore, in the optical regime, the GNPs have only very limited loss at Dirac point because of their outstanding optical characteristics, including ballistic transport and saturable absorption [25–28]. Therefore, GNPs can be easily and successfully incorporated with polymeric matrices to enhance the comprehensive performance of polymers. As for PCMs, it has already been demonstrated that the addition of even a small mass fraction of GNPs can significantly improve the thermal conductivity of different PCMs such as palmitic acid [23,29], beeswax [12], eicosane [30], 1-octadecanol [31], decosane [32]. In addition, the rheological behavior of PCMs can be significantly influenced by the addition of nanoplates, which determines the

transportability in pump systems for PCMs nanofluids applications. However, in previous literatures, the comprehensive effects of GNPs on the thermal conductivity, rheological behavior, and optical absorption performance of PCMs are hardly explored together, hence, this work will focus on analyzing the three effects.

In this paper, a series of PEG/GNPs composites were prepared through a temperature-assisted solution blending method in order to develop new PCMs for utilizing solar energy. The good compatibility between PEG and GNPs conduce to excellent thermal conductivity and high latent heat at low filler mass fraction. Furthermore, the composites exhibit a better performance in absorbing and conversing solar energy in comparison with the traditional organic PCMs. Therefore, the outstanding thermal conductivity and photothermal performance make the PEG/GNPs composites a promising candidate for solar thermal energy storage application.

## 2. Experimental

### 2.1. Materials

PEG (Mn = 4000), as the latent heat storage material, was purchased from Chengdu Kelong Chemical Reagent Factory (Chengdu, China). GNP nanoplates (Grade C750) (Thickness: <2 nm, Width: <2  $\mu\text{m}$ , Specific surface area: 750  $\text{m}^2/\text{g}$ , purity: >99%) were purchased from XG Science (Lansing, MI, USA). Ethanol was obtained from Chongqing Chuandong Chemical Group (Chongqing, China). All the materials were of analytical grade.

### 2.2. Preparation of the PEG/GNPs Composites

PEG/GNPs composites were prepared by the temperature-assisted solution blending method. Firstly, GNPs were dispersed in ethanol in aid of ultrasonication for 1 h to form a homogeneous suspension, meanwhile, the PEG was heated by water bath at 80 °C in a beaker. Then the GNPs suspension was slowly dropped into melted liquid PEG and the hybrid solution was stirred vigorously for 4 h under the same conditions to evaporate the remaining ethanol. Finally, the products were dried in a vacuum oven to a constant weight at 60 °C. For comparison purposes, pristine PEG was also prepared with the same procedure. Here, the mass fraction of GNPs in PEG/GNPs composites varied from 0.5 to 2% (0.5, 1, 1.5 and 2 wt %), for convenience, the obtained samples were labeled as PEG/GNPs-X%, where X was characteristic of the GNPs mass fraction in the composites.

### 2.3. Characterization

A EVO18 scanning electron microscope (SEM) instrument (CARL ZEISS, Oberkochen, Germany) was used to visually characterize the morphology of the composites with an accelerating voltage of 20 kV. All samples were sputtered with gold prior to test.

Fourier transform infrared (FT-IR) spectra of PEG, GNPs, and PEG/GNPs composites were performed on a Nicolet 6700 (Nicolet Instrument Company, Waltham, MA, USA) at the wavenumber range of 4000–500  $\text{cm}^{-1}$ .

The crystal structures and crystallization characteristic of PEG in composites was explored by X'Pert Powder model of X-ray diffractometer (PANalytical B.V., Almelo, the Netherlands) with Cu K $\alpha$  radiation ( $\lambda = 0.154 \text{ nm}$ ) under a voltage of 40 kV and a current of 40 mA. The scanning angle  $2\theta$ , from 10° to 40° at a scanning speed of 3°/min.

The thermal energy storage properties of the composites were investigated using a differential scanning calorimeter (DSC) (DSC6000, Perkin-Elmer Inc., Waltham, Mass, USA) at a heating and cooling rate of 10°/min under a constant stream of nitrogen. This process was repeated for the three heating-cooling cycles and the third one was used to analyze the result.

The UV-VIS-NIR spectroscopy was performed on a UV-3600 spectrophotometer (SHIMADZU, Tokyo, Japan).

The thermal conductivity of the samples was measured using a LFA 447 MicroFlash Apparatus (Netzsch, SELB, Germany) by the Laser Flash method. To ensure the accuracy of the measurement, the thermal conductivity of each sample was measured five times.

The viscosity of the composites was tested using a viscometer (DVDV-I, Brookfield, Middleboro, MA, USA) with accuracy within  $\pm 1\%$ .

The light-to-thermal energy conversion experiment was conducted using a 300 W solar simulator (ULTRA-VITALUX, OSRAM, Munich, Germany) as the light source. During the test, the temperatures of the samples were recorded using a L93-6 temperature logger with thermocouples (Hangzhou Loggertech Co., Ltd., Zhejiang, China).

### 3. Result and Discussion

#### 3.1. Microstructure Analysis

The microstructures of the GNPs, pristine PEG and PEG/GNPs-2% composite are shown in Figure 1. The GNPs in Figure 1a exhibit wrinkled surface textures with curling edges, and they are especially prone to agglomerate because of their high specific surface areas and strong  $\pi$ - $\pi$  interaction. Actually, these wrinkled surface with a lot of creases can play a positive role in enhancing the strong interaction between GNPs with PEG. For pristine PEG, a relatively smooth surface and compact structure appears (Figure 1b), completely different from that of GNPs. The morphology of the PEG/GNPs composite is shown in Figure 1c, as can be seen, the surface of PEG displays a conspicuous change that appears to be rougher than that of pure PEG, which may be attributed to the uniform dispersion of GNPs in the PEG matrix. The composite presents a coarse surface with plenty of creases stacking layer by layer, which seems to provide a network-like structure that the phonons can efficiently travel along and accelerate heat transfer, thus, there will be a significant enhancement in the thermal conductivity of composites in comparison with that of pure PEG [31]. Moreover, Figure 1b,c confirm the suitable interactions and desirable compatibility between GNPs and PEG matrix because of the van der Waals force, hydrophobic-hydrophobic interaction and  $\pi$ - $\pi$  interaction [24,33]. Therefore, it can be demonstrated that the GNPs can be used as a kind of filler material for the fabrication of PEG with remarkable thermal conductivity at a low loading ration.

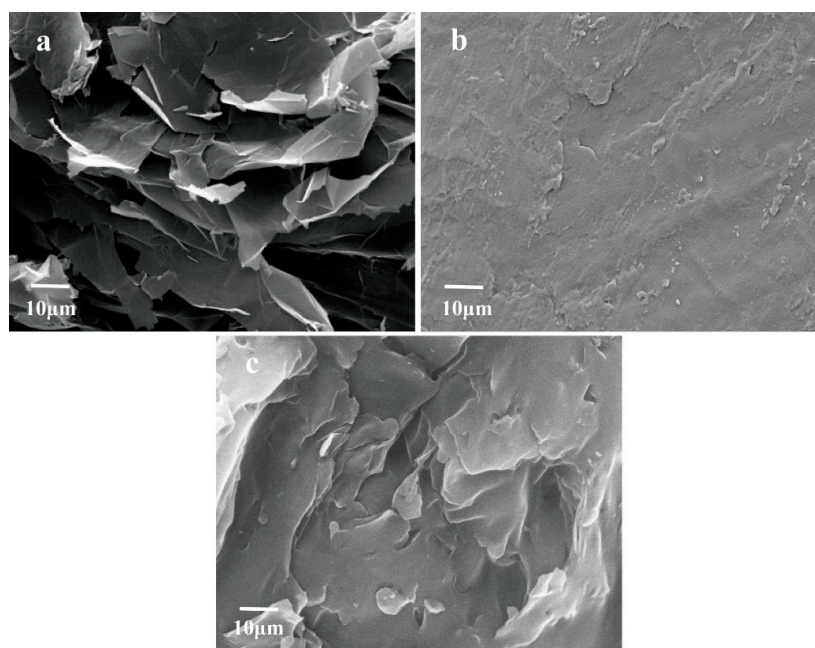


**Figure 1.** Scanning electron microscope (SEM) images of the graphene nanoplatelets (GNPs) (a), pristine polyethylene glycol (PEG) (b) and PEG/GNPs-2% composite (c).

### 3.2. FT-IR Analysis

The chemical compatibility of the PEG/GNPs composites was characterized by FT-IR spectroscopy (Figure 2). As shown in Figure 2, in the spectrum of pure PEG, the absorption peak at  $3435\text{ cm}^{-1}$  belongs to the stretching vibration of O–H groups while the sharp peak at  $2881\text{ cm}^{-1}$  is attributed to the C–H stretching vibration. Moreover, the obtained bands at  $1642\text{ cm}^{-1}$  and  $1110\text{ cm}^{-1}$  represent the C=O stretching vibration and C–O asymmetric stretching vibration, respectively. In addition, the C–H bending vibration is shown at  $841\text{ cm}^{-1}$ . Similar observations were reported in a previous study [34]. In terms of the spectrum of GNPs, it appears nearly a flat line because it is universally acknowledged that there are few functional groups on GNPs [18]. It can be clearly seen that the absorption peaks in the spectrum of PEG/GNPs composites are in accordance with the spectrum of PEG, which reveals that the previously mentioned peaks of PEG remain constant in the composites. Furthermore, no distinct new peaks are observed in the spectra of the mixtures, suggesting that there are only physical reactions between PEG and GNPs rather than chemical reactions.

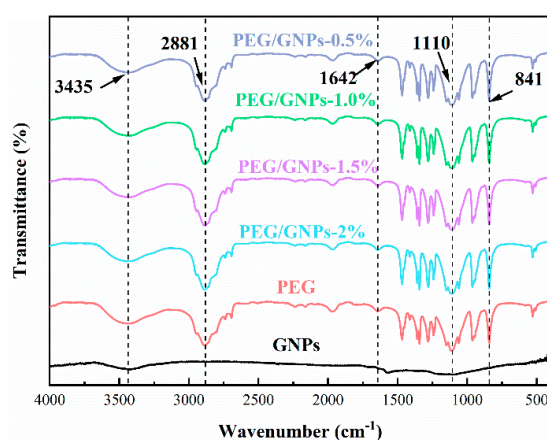


**Figure 2.** Fourier transform infrared (FT-IR) spectra of GNPs, pure PEG and PEG/GNPs composites with different contents of GNPs.

### 3.3. X-ray Diffraction (XRD) Analysis

Figure 3 presents the XRD patterns of the pure PEG, GNPs and PEG/GNPs composites. The low intensity diffraction peak at  $26.23^\circ$  is the main peak of GNPs, which reveals the random stacking of a few of graphene sheets and represents the crystallization of GNPs [23]. The two sharp diffraction peaks of the PEG appeared at  $19.06^\circ$  and  $23.17^\circ$ , which indicates a polymer with high crystallinity. After GNPs are uniformly dispersed into the PEG matrix, the typical diffraction peaks of PEG can still be observed and the peak positions do not change. However, the characteristic peak of the GNPs is not shown in the PEG/GNPs composites, which can be ascribed to the fact that the GNPs loading is extremely low compared to that of PEG. On the other hand, the peak intensities of PEG slightly changed after the incorporation of GNPs, especially for the peak at  $23.17^\circ$ . For the composites, the intensities of peaks at  $23.17^\circ$  are relatively lower than that of pristine PEG when the content of GNPs varies from 0.5% to 1.5%. The possible reason is that the strong interaction between GNPs and PEG can restrict the mobility of PEG molecular chains, resulting in the decrease in crystallization of PEG. Therefore, from the XRD results, it can be confirmed that the PEG/GNPs composites can still possess well-maintained crystallization behaviors, and there is no significant effect of the GNPs on the crystal structure of the pure PEG. Moreover, the XRD results can be seen as an indication that no chemical reaction between GNPs and PEG occur.

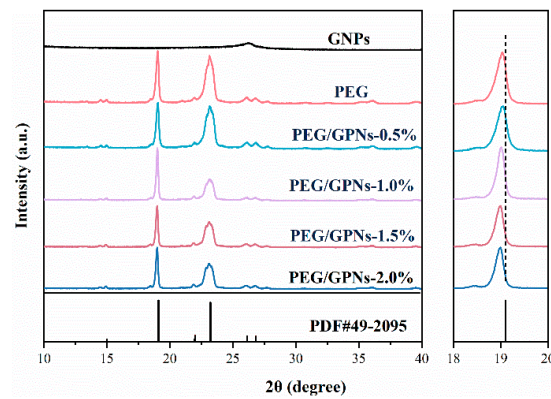


**Figure 3.** X-ray diffraction (XRD) patterns of GNPs, pure PEG and PEG/GNPs composites with the different contents of GNPs.

#### 3.4. Thermal Storage Performance Analysis

The phase change temperature and thermal energy storage properties of pristine PEG and PEG/GNPs composites were measured by the DSC technique to explore the effect of GNPs on the thermal storage performance of composites. The melting and solidifying DSC curves of PEG and PEG/GNPs composites are shown in Figures 4 and 5, respectively. The detailed calorimetric results of the DSC experiments are tabulated in Table 1, including starting melting/solidifying temperature ( $T_{ms}/T_{ss}$ ), end melting/solidifying temperature ( $T_{me}/T_{se}$ ), peak melting/solidifying temperature ( $T_{mp}/T_{sp}$ ), endothermic/exothermic enthalpy ( $\Delta H_m/\Delta H_c$ ). Obviously, for all samples, the conspicuous endothermic and exothermic peak are both exhibited in the melting and solidifying process, which represent the solid-liquid phase change of the pure PEG. As can be observed from Table 1, compared with pristine PEG, the  $T_s$  of the composites is not significantly influenced by the addition of GNPs. Notably, the composites present lower melting temperatures than that of pure PEG, which is possible attributed to the incorporation of GNPs. When the GNPs are uniformly dispersed into the PEG matrix, the intimate interaction between GNPs and PEG, such as surface tension forces,  $\pi$ - $\pi$  interactions, and capillary forces, will confine the mobility of PEG molecules, resulting in the decline of phase change temperature. Additionally, the thermal conductivity of composites can be enhanced significantly with the addition of GNPs, which leads to a rapid thermal response. Similar results were founded in a previous study [34]. Therefore, it is demonstrated that the decrease in  $T_m$  between pure PEG and composites can be ascribed to the comprehensive effects of these factors.

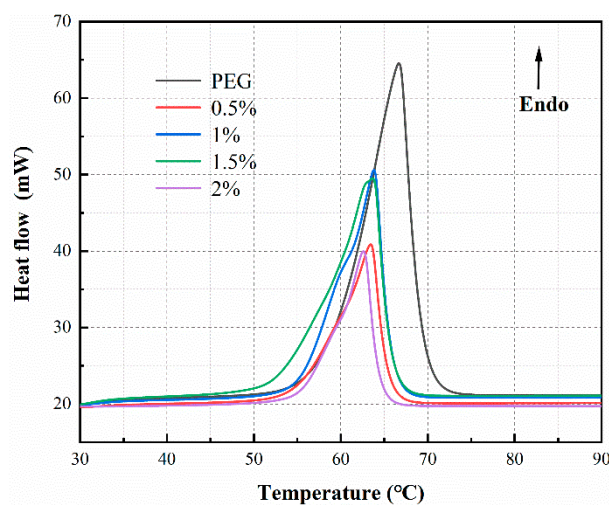


**Figure 4.** Melting differential scanning calorimeter (DSC) curves of the pure PEG and PEG/GNPs composites with the different contents of GNPs.

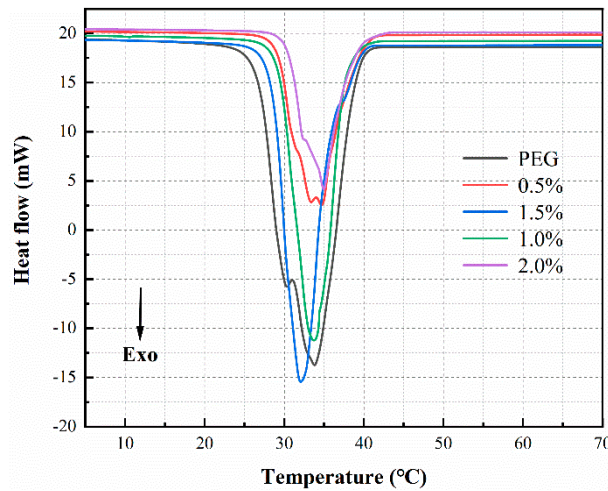


**Figure 5.** Solidifying DSC curves of the pure PEG and PEG/GNPs composites with the different contents of GNPs.

**Table 1.** DSC melting and solidifying characteristics of pristine PEG and PEG/GNPs-X% composites.

Sample	$T_{ms}$ (°C)	$T_{mp}$ (°C)	$T_{me}$ (°C)	$\Delta H_m$ (J/g)	$T_{ss}$ (°C)	$T_{sp}$ (°C)	$T_{se}$ (°C)	$\Delta H_s$ (J/g)
PEG	58.8	66.9	69.1	180.7	38.9	33.8	27.5	161.3
PEG/GNPs-0.5%	57.5	63.8	65.9	178.5	37.6	34.6	29.3	158.4
PEG/GNPs-1%	57.9	63.4	65.7	175.2	36.4	33.7	29.4	155.6
PEG/GNPs-1.5%	56.4	63.2	65.6	172.1	36.5	32.1	28.6	152.8
PEG/GNPs-2%	56.1	62.6	64.8	170.6	37.1	34.2	29.5	151.3

High latent heat is an imperative factor in PCMs, since it is directly related to the capacity of PCMs for energy storage. As can be seen in Table 1, the  $\Delta H_m$  of the composites decrease with the increasing mass fraction of the GNPs. One reason for this latent heat loss is that some of the PEG volume is replaced by the GNPs, which do not undergo a phase change. Moreover, it is noticeable that the measured latent heat values of the composites in the process of melting are slightly lower than the arithmetically calculated values by the following equation:

$$\Delta H_{\text{nano-composite}} = \mu \times \Delta H_{\text{PEG}} \tag{1}$$

where  $\Delta H_{\text{nano-composites}}$  is the calculated latent heat value of the PEG/GNPs composite,  $\mu$  and  $\Delta H_{\text{PEG}}$  are the PEG weight percentage of composite and the latent heat of pure PEG, respectively. The measured and calculated latent heat of the composites in the process of melting are compared in Table 2. As can be seen, the relative errors between the measured and calculated values have a tendency to increase with the increasing mass fraction of GNPs. The measured latent heat capacity of the composites doped with 2 wt. % GNPs are 4.4% lower when compared to the calculated values. This possibility is ascribed to the physical interactions between GNPs and PEG, such as van der Waals force and hydrophobic-hydrophobic interaction, which can restrict the mobility of PEG molecular chains during the process of crystallization, as a result, the phase change enthalpy of PEG decreases [34]. We did not increase the GNPs mass fraction beyond 2 wt. % to avoid further decrease in the latent melting heat. The effect of GNPs content to thermal storage performance is shown in Figure 6. As the GNPs content increases, the latent heat gradually decreases while the thermal conductivity increases, implying that the enhancement of thermal conductivity using GNPs will be accompanied by decreased latent heat in the composites. Whereas adding 2 wt. % GNPs results in a 146% increase in thermal conductivity and only a 6.3% reduction in the latent heat of the PEG used in the current work. Therefore, it may be beneficial to add a low loading ration of GNPs to obtain the suitable latent heat as well as enhance the thermal conductivity of composites.

**Table 2.** Calculated and measured values of the melting latent heat of composites.

Mass Fraction of GNPs (%)	The Calculated Latent Heat (J/g)	The Measured Latent Heat (J/g)	The Relative Errors (%)
0.5	179.8	178.5	0.7
1.0	178.9	175.2	2.1
1.5	178.0	172.1	3.1
2.0	177.1	169.3	4.4

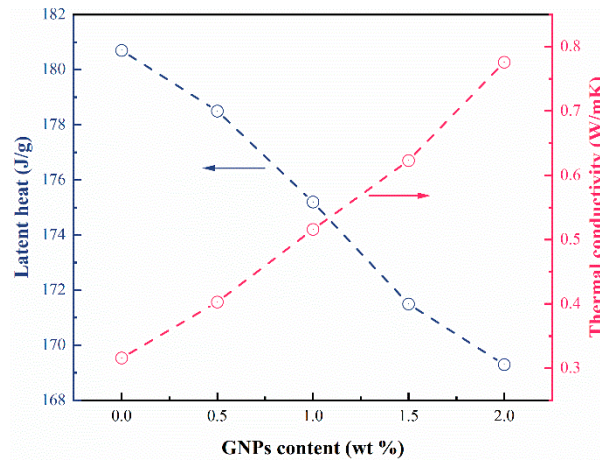


**Figure 6.** The latent heat and thermal conductivity of the composite as a function of GNPs contents.

### 3.5. Thermal Conductivity Analysis

The thermal conductivity results of PEG and PEG/GNPs composites are shown in Figure 7. The thermal conductivity of PEG is only 0.316 W/mK, which fails to meet the requirements for efficient thermal storage application. Impressively, it is seen that the thermal conductivities of PEG/GNPs composites increase remarkably as the GNPs weight fraction increases. The thermal conductivity of the composite doped with 2.0 wt % GNPs (PEG/2GNPs) is measured to be as high as 0.776 W/mK, exhibiting a relative increment of above 146%. Moreover, the figure illustrates that the thermal conductivity has a tendency to ascend, implying that GNPs are excellent additives for improving the thermal conductivity of PEG.

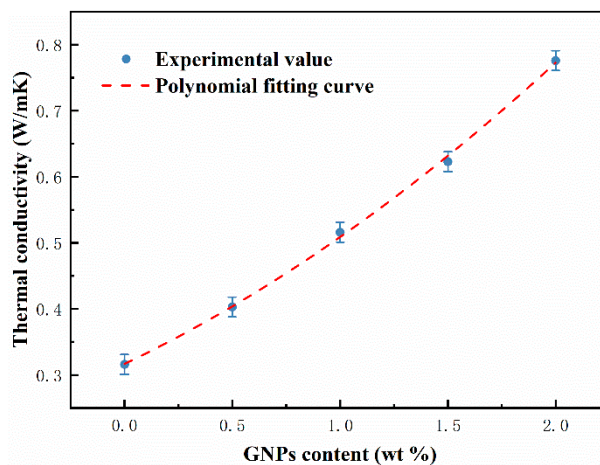


**Figure 7.** Thermal conductivity of the composites with different contents of GNPs.

GNPs dispersing in PEG matrix can form uniformly aqueous system when the mass fraction of GNPs is relatively low in aid of magnetic stirring and ultrasonic bath. Thus, at a certain filling rate, the different layers of graphene nanoplates interact effectively with each other, forming a high thermal

conductivity network. Moreover, the large specific surface area of GNPs greatly reduces the interfacial thermal resistance between the GNPs and PEG matrix materials, as a result, heat will rapidly transfer among GNPs instead of through the PEG matrix. Yu et al. [35] and Fan et al. [36] point out that the low interfacial thermal resistance provided by GNPs is ascribed to the reduced geometric contribution of phonon scattering at the interfaces.

In this work, the polynomial fitting curve is aimed at demonstrating the relationship between thermal conductivity of the PEG/GNPs and the content of GNPs. The dotted red line in Figure 7 represents the polynomial fitting curve, and the relation is expressed as following:

$$\gamma = 0.3168 + 0.156x + 0.036x^2 \quad (2)$$

where  $\gamma$  is thermal conductivity of the composites,  $x$  represents the content of GNPs. The coefficient of correlation of the Equation (2) is 0.998, which exhibits a high correlation between the thermal conductivity of composites and the content of GNPs.

High thermal conductivity is a significant element considered for the advanced thermal energy and heat transfer of PCMs. Thus, the enhanced heat transfer rates of PEG/GNPs composites were further investigated. A temperature recorder with thermocouples was used to record the melting and solidifying times for the purpose of evaluating the temperature response behavior of the composites. Before the test, the sample was heated to 90 °C in the 20 mL tube, then the thermocouple was inserted into the middle of the sample, finally, the sample cooled down to room temperature and contacted closely with the thermocouple. The temperature-time profiles of the pristine PEG and composites for both the processes are illustrated in Figure 8. In the melting process, it can be vividly observed that the rising rate of temperature is significantly much faster in PEG/GNPs-2% composite. In addition, the peak temperature of PEG/GNPs-2% reaches 74.9 °C, higher than that of PEG. It is clearly revealed that the GNPs can accelerate the conductivity thermal transfer during the heating process. Then the tubes were immediately put into another thermostatic water baths with the constant temperature of 25 °C. Expectedly, the temperature of pristine PEG continuously decreases at lower rate than that of PEG/GNPs-2% composite due to the different capacity of conductivity thermal transfer. For instance, from the curves depicted in Figure 8, the times taken by pure PEG and PEG/GNPs-2% composite for decreasing to 30 °C from the peak temperatures are determined as about 545 s and 1665 s, respectively, indicating that the composites are more efficient in storing and releasing thermal energy. The faster melting and solidifying rates demonstrate that the thermal conductivity of composites can be significantly promoted by adding the GNPs. From the results mentioned above, it is confirmed that the PEG/GNPs composite has the potential for effective thermal energy management.

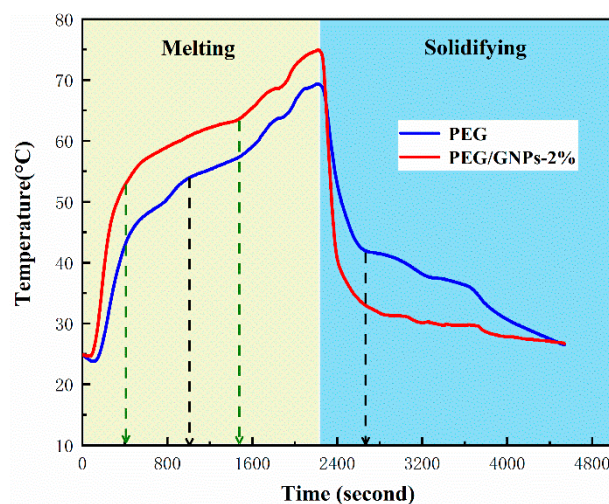


**Figure 8.** Heating and cooling-rate curves of pure PEG and PEG/GNPs-2% composites.

### 3.6. Rheological Behavior Analysis

To investigate the rheological behavior of PEG/GNPs composites during the phase change process, a Brookfield DVDV-I viscometer was used to measure the viscosity of the composite fluids at a constant shear stress. The composites were melted before being poured into the sample catcher, and the thermostatic water baths were set to 70 °C to keep the PEG/GNPs composites in the liquid phase. Figure 9 illustrates the viscosity of the composites with different concentrations of GNPs using the ratio method. As can be seen, the viscosity of the composites exhibit a tendency to increase with increasing the mass fraction of GNPs in agreement with other studies [37]. For example, when the loaded GNPs content increases from 0% to 2%, the viscosity of the PEG/GNPs composite fluid increases from 0.11 cP to 0.32 cP at the same temperature, showing a 190.1% enhancement in viscosity compared to the PEG base fluid. It is indicated that the addition of GNPs can increase the viscosity of PEG fluid, which can be attributed to the larger interfacial area of the GNPs with a greater mass fraction in the fluid, and the increase in frictional forces among the GNPs of a larger number [38]. Amin et al. [12] obtained the similar results, showing that the viscosity of PCMs nanofluids can be enhanced by the addition of nanoplates.

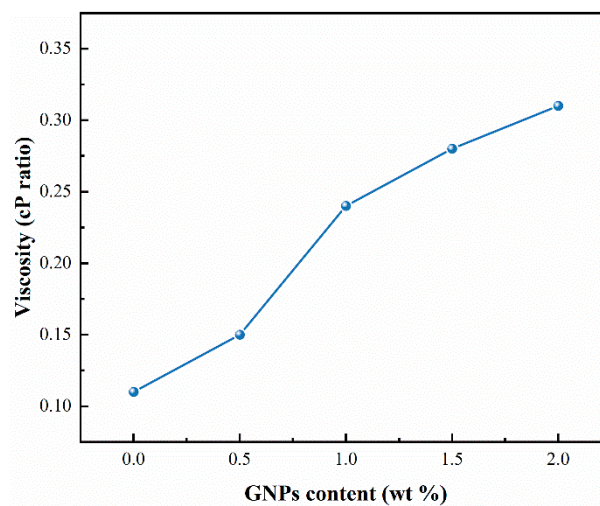


**Figure 9.** Viscosity of the composites with different contents of GNPs.

### 3.7. Photothermal Conversion Performance Analysis

To evaluate whether the PEG/GNPs composites are capable of absorbing and converting solar energy more effectively in comparison with pristine PEG when exposed to solar irradiation, we designed an experimental apparatus to conduct the photothermal conversion experiments on them, which was composed of two parts: photothermal conversion system and data acquisition system. The first system consisted of an insulated chamber, serial thermometer, temperature control device, temperature-sensing device, and a light source. The second system consisted of temperature logger with several thermocouples and a computer. Prior to testing, the sample melted at 85 °C was poured into a quartz beaker, then the thermocouple was put in the middle of the sample. During the process of cooling, it is imperative to keep the thermocouple in the correct position to ensure close contact with the sample. The variations in temperature of pristine PEG and PEG/GNPs-2% composite with the irradiation time are depicted in Figure 10. As can be observed, during the light irradiation period, the PEG/GNPs-2% composite can fully absorb and convert the light energy, as a result, the temperature exhibits a rapid rising trend. When the temperature achieves the melting value of the composite, a turning point appears in the temperature variation curve, indicating that the composite begins to process a phase change and store energy. After the illumination is removed, the temperature of the composite starts to decline, and the curve shows a constant temperature heat release platform, which indicates that the composite begins to crystallize. However, the temperature of pristine PEG

risers slowly and barely reaches its melting point, exhibiting a low efficiency in utilizing the light energy. Therefore, compared with pure PEG, the PEG/GNPs nanocomposites show better performance in photothermal energy conversion.

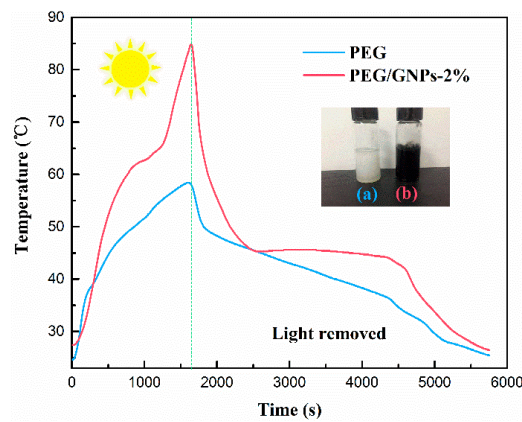


**Figure 10.** The variation in temperature with irradiation time of pure PEG and PEG/GNPs-2% composite.

To illustrate the reasons for the higher absorption efficiency of PEG/GNPs for solar irradiation compared with pure PEG, the Ultraviolet-visible-Near Infrared spectroscopy was used to measure the diffuse reflection spectra of PEG and PEG/GNPs composites. As shown in the Figure 11, the light absorption performance of PEG/GNPs composite is obviously much higher than that of pristine PEG in throughout at 200 to 2000 nm wavelength, suggesting that the PEG doped with GNPs make an outstanding increase in the solar light absorbance characteristic. Furthermore, the composite shows one total absorbance property in the different spectral region, which is essential to utilize the solar thermal energy to the greatest extent. This possibly can be attributed to a zero-bandgap structure of GNPs, which can theoretically absorb any wavelength, in addition, when the intensity of the incident light exceeds a certain threshold, the absorption of GNPs will reach saturation. As can be seen from photograph (inset in Figure 10), compared with PEG/GNPs composite, the pristine PEG has a white surface which can form a reflective layer that hinders the absorption of solar light. Accordingly, compared with pure PEG, the PEG/GNPs composites exhibit higher conductivity and better solar radiation absorption capacity, resulting in the more excellent performance in photothermal energy conversion. Therefore, the PEG/GNPs composites are expected to have great potential for solar energy conversion with respect to their better thermal conductivity and photothermal performance.

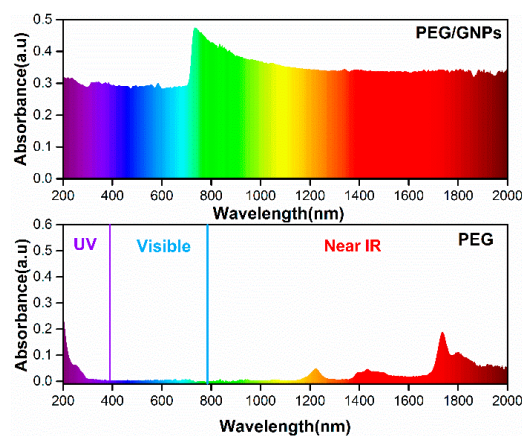


**Figure 11.** The Ultraviolet-visible-Near Infrared diffuse reflection spectra of pure PEG and PEG/GNPs-2% composite.

#### 4. Conclusions

The PEG/GNPs nanocomposites with various contents of GNPs have been successfully prepared with the objective of investigating the enhanced thermal conductivity and photothermal performance of this nanocomposites. Samples of the PEG/GNPs nanocomposites were synthesized using a temperature-assisted solution blending method. SEM reveal that the GNPs are uniformly dispersed in the PEG matrix and construct a heat conduction way. FT-IR and XRD analysis show that no chemical interaction between PEG and GNPs happen, in addition, the suitable content of GNPs can promote the crystallization of PEG. The DSC results show that the phase change temperature and enthalpy are slightly influenced by GNPs content. In addition, the thermal conductivity of the composites is remarkably enhanced by the addition of GNPs, and adding 2 wt. % GNPs results in 146% increase in thermal conductivity and only 6.3% reduction in the latent heat of the PEG. The photothermal conversion performance of the PEG/GNPs nanocomposites is higher than that of pure PEG, which is ascribed to the nanocomposites possess better thermal conductivity and excellent visible light absorptivity in comparison with the pure PEG. The enhanced thermal conductivity property and photothermal conversion performance make the PEG/GNPs nanocomposites very promising for the application of solar energy conversion and storage.

**Author Contributions:** Data curation, H.W. and Y.G.; Formal analysis, X.L.; Investigation, H.W.; Methodology, H.W. and H.Z.; Resources, X.M.; Software, H.W.; Supervision, L.H.; Writing—original draft, H.W.; Writing—review & editing, H.W.

**Funding:** This work was jointly supported by National Natural Science Foundation of China (Grant Nos. 51508063, 51506018), the Science and Technology Research Program of Chongqing Municipal Education Commission (Grant No. KJ1705145).

**Acknowledgments:** The authors would like to express gratitude to thank the reviewers and editor for kindly giving revising suggestions.

**Conflicts of Interest:** The authors declare no conflicts of interest.

#### References

1. Karaipekli, A.; Biçer, A.; Sarı, A.; Tyagi, V.V. Thermal characteristics of expanded perlite/paraffin composite phase change material with enhanced thermal conductivity using carbon nanotubes. *Energy Convers. Manag.* **2017**, *134*, 373–381. [[CrossRef](#)]
2. Barlev, D.; Vidu, R.; Stroeve, P. Innovation in concentrated solar power. *Sol. Energy Mater. Sol. Cells* **2011**, *95*, 2703–2725. [[CrossRef](#)]
3. Granqvist, C.G. Transparent conductors as solar energy materials: A panoramic review. *Sol. Energy Mater. Sol. Cells* **2007**, *91*, 1529–1598. [[CrossRef](#)]
4. Crabtree, G.W.; Lewis, N.S. Solar energy conversion. *Dalton Trans.* **2009**, *60*, 37–42.
5. Zeng, J.-L.; Zheng, S.-H.; Yu, S.-B.; Zhu, F.-R.; Gan, J.; Zhu, L.; Xiao, Z.-L.; Zhu, X.-Y.; Zhu, Z.; Sun, L.-X.; et al. Preparation and thermal properties of palmitic acid/polyaniline/exfoliated graphite nanoplatelets form-stable phase change materials. *Appl. Energy* **2014**, *115*, 603–609. [[CrossRef](#)]
6. Khan, Z.; Khan, Z.; Ghafoor, A. A review of performance enhancement of PCM based latent heat storage system within the context of materials, thermal stability and compatibility. *Energy Convers. Manag.* **2016**, *115*, 132–158. [[CrossRef](#)]
7. Qi, G.-Q.; Liang, C.-L.; Bao, R.-Y.; Liu, Z.-Y.; Yang, W.; Xie, B.-H.; Yang, M.-B. Polyethylene glycol based shape-stabilized phase change material for thermal energy storage with ultra-low content of graphene oxide. *Sol. Energy Mater. Sol. Cells* **2014**, *123*, 171–177. [[CrossRef](#)]
8. Fang, G.; Li, H.; Chen, Z.; Liu, X. Preparation and properties of palmitic acid/SiO<sub>2</sub> composites with flame retardant as thermal energy storage materials. *Sol. Energy Mater. Sol. Cells* **2011**, *95*, 1875–1881. [[CrossRef](#)]
9. Agyenim, F.; Hewitt, N.; Eames, P.; Smyth, M. A review of materials, heat transfer and phase change problem formulation for latent heat thermal energy storage systems (LHTESS). *Renew. Sustain. Energy Rev.* **2010**, *14*, 615–628. [[CrossRef](#)]

10. Kaizawa, A.; Kamano, H.; Kawai, A.; Jozuka, T.; Senda, T.; Maruoka, N.; Akiyama, T. Thermal and flow behaviors in heat transportation container using phase change material. *Energy Convers. Manag.* **2008**, *49*, 698–706. [[CrossRef](#)]
11. Yang, J.; Qi, G.-Q.; Liu, Y.; Bao, R.-Y.; Liu, Z.-Y.; Yang, W.; Xie, B.-H.; Yang, M.-B. Hybrid graphene aerogels/phase change material composites: Thermal conductivity, shape-stabilization and light-to-thermal energy storage. *Carbon* **2016**, *100*, 693–702. [[CrossRef](#)]
12. Amin, M.; Putra, N.; Kosasih, E.A.; Prawiro, E.; Luanto, R.A.; Mahlia, T.M.I. Thermal properties of beeswax/graphene phase change material as energy storage for building applications. *Appl. Therm. Eng.* **2017**, *112*, 273–280. [[CrossRef](#)]
13. Wu, W.F.; Liu, N.; Cheng, W.L.; Liu, Y. Study on the effect of shape-stabilized phase change materials on spacecraft thermal control in extreme thermal environment. *Energy Convers. Manag.* **2013**, *69*, 174–180. [[CrossRef](#)]
14. He, L.; Li, J.; Zhou, C.; Zhu, H.; Cao, X.; Tang, B. Phase change characteristics of shape-stabilized PEG/SiO<sub>2</sub> composites using calcium chloride-assisted and temperature-assisted sol gel methods. *Sol. Energy* **2014**, *103*, 448–455. [[CrossRef](#)]
15. Sari, A.; Alkan, C.; Biçer, A. Synthesis and thermal properties of polystyrene-graft-PEG copolymers as new kinds of solid–solid phase change materials for thermal energy storage. *Mater. Chem. Phys.* **2012**, *133*, 87–94. [[CrossRef](#)]
16. Alkan, C.; Günther, E.; Hiebler, S.; Himpel, M. Complexing blends of polyacrylic acid-polyethylene glycol and poly(ethylene-co-acrylic acid)-polyethylene glycol as shape stabilized phase change materials. *Energy Convers. Manag.* **2012**, *64*, 364–370. [[CrossRef](#)]
17. Onder, E.; Sarier, N.; Ukuser, G.; Ozturk, M.; Arat, R. Ultrasound assisted solvent free intercalation of montmorillonite with PEG1000: A new type of organoclay with improved thermal properties. *Thermochim. Acta* **2013**, *566*, 24–35. [[CrossRef](#)]
18. Tang, Y.; Jia, Y.; Alva, G.; Huang, X.; Fang, G. Synthesis, characterization and properties of palmitic acid/high density polyethylene/graphene nanoplatelets composites as form-stable phase change materials. *Sol. Energy Mater. Sol. Cells* **2016**, *155*, 421–429. [[CrossRef](#)]
19. Deng, Y.; Li, J.; Qian, T.; Guan, W.; Li, Y.; Yin, X. Thermal conductivity enhancement of polyethylene glycol/expanded vermiculite shape-stabilized composite phase change materials with silver nanowire for thermal energy storage. *Chem. Eng. J.* **2016**, *295*, 427–435. [[CrossRef](#)]
20. Zhang, X.; Huang, Z.; Ma, B.; Wen, R.; Zhang, M.; Huang, Y.; Fang, M.; Liu, Y.; Wu, X. Polyethylene glycol/Cu/SiO<sub>2</sub> form stable composite phase change materials: Preparation, characterization, and thermal conductivity enhancement. *RSC Adv.* **2016**, *6*, 58740–58748. [[CrossRef](#)]
21. Harikrishnan, S.; Magesh, S.; Kalaiselvam, S. Preparation and thermal energy storage behaviour of stearic acid–TiO<sub>2</sub> nanofluids as a phase change material for solar heating systems. *Thermochim. Acta* **2013**, *565*, 137–145. [[CrossRef](#)]
22. Cataldi, P.; Athanassiou, A.; Bayer, I. Graphene Nanoplatelets-Based Advanced Materials and Recent Progress in Sustainable Applications. *Appl. Sci.* **2018**, *8*, 1438. [[CrossRef](#)]
23. Silakhori, M.; Fauzi, H.; Mahmoudian, M.R.; Metselaar, H.S.C.; Mahlia, T.M.I.; Khanlou, H.M. Preparation and thermal properties of form-stable phase change materials composed of palmitic acid/polypyrrole/graphene nanoplatelets. *Energy Build.* **2015**, *99*, 189–195. [[CrossRef](#)]
24. Hu, K.; Kulkarni, D.D.; Choi, I.; Tsukruk, V.V. Graphene-polymer nanocomposites for structural and functional applications. *Prog. Polym. Sci.* **2014**, *39*, 1934–1972. [[CrossRef](#)]
25. Pu, M.; Chen, P.; Wang, Y.; Zhao, Z.; Wang, C.; Huang, C.; Hu, C.; Luo, X. Strong enhancement of light absorption and highly directive thermal emission in graphene. *Opt. Express* **2013**, *21*, 11618–11627. [[CrossRef](#)]
26. Novoselov, K.S.; Geim, A.K.; Morozov, S.V.; Jiang, D.; Katsnelson, M.I.; Grigorieva, I.V.; Dubonos, S.V.; Firsov, A.A. Two-dimensional gas of massless Dirac fermions in graphene. *Nature* **2005**, *438*, 197. [[CrossRef](#)]
27. Nilsson, J.; Neto, A.H.; Guinea, F.; Peres, N.M. Electronic properties of graphene multilayers. *Phys. Rev. Lett.* **2006**, *97*, 266801. [[CrossRef](#)]
28. Nair, R.R.; Blake, P.; Grigorenko, A.N.; Novoselov, K.S.; Booth, T.J.; Stauber, T.; Peres, N.M.; Geim, A.K. Fine structure constant defines visual transparency of graphene. *Science* **2008**, *320*, 1308. [[CrossRef](#)]
29. Mehrali, M.; Latibari, S.T.; Mehrali, M.; Mahlia, T.M.I.; Metselaar, H.S.C.; Naghavi, M.S.; Sadeghinezhad, E.; Akhiani, A.R. Preparation and characterization of palmitic acid/graphene nanoplatelets composite with remarkable thermal conductivity as a novel shape-stabilized phase change material. *Appl. Therm. Eng.* **2013**, *61*, 633–640. [[CrossRef](#)]

30. Fang, X.; Fan, L.W.; Ding, Q.; Wang, X.; Yao, X.L.; Hou, J.F.; Yu, Z.T.; Cheng, G.H.; Hu, Y.C.; Cen, K.F. Increased Thermal Conductivity of Eicosane-Based Composite Phase Change Materials in the Presence of Graphene Nanoplatelets. *Energy Fuels* **2013**, *27*, 4041–4047. [[CrossRef](#)]
31. Yavari, F.; Fard, H.R.; Pashayi, K.; Rafiee, M.A.; Zamiri, A.; Yu, Z.; Ozisik, R.; Borcatasciuc, T.; Koratkar, N. Enhanced Thermal Conductivity in a Nanostructured Phase Change Composite due to Low Concentration Graphene Additives. *J. Phys. Chem. C* **2011**, *115*, 8753–8758. [[CrossRef](#)]
32. Li, J.F.; Lu, W.; Zeng, Y.B.; Luo, Z.P. Simultaneous enhancement of latent heat and thermal conductivity of docosane-based phase change material in the presence of spongy graphene. *Sol. Energy Mater. Sol. Cells* **2014**, *128*, 48–51. [[CrossRef](#)]
33. Su, Q.; Pang, S.; Alijani, V.; Li, C.; Feng, X.; Müllen, K. Composites of Graphene with Large Aromatic Molecules. *Adv. Mater.* **2009**, *21*, 3191–3195. [[CrossRef](#)]
34. He, L.; Wang, H.; Yang, F.; Zhu, H. Preparation and properties of polyethylene glycol/unsaturated polyester resin/graphene nanoplates composites as form-stable phase change materials. *Thermochim. Acta* **2018**, *665*, 43–52. [[CrossRef](#)]
35. Yu, A.; Ramesh, P.; Itkis, M.E.; Elena Bekyarova, A.; Haddon, R.C. Graphite Nanoplatelet—Epoxy Composite Thermal Interface Materials. *J. Phys. Chem. C* **2007**, *111*, 7565–7569. [[CrossRef](#)]
36. Yu, Z.T.; Fang, X.; Fan, L.W.; Wang, X.; Xiao, Y.Q.; Zeng, Y.; Xu, X.; Hu, Y.C.; Cen, K.F. Increased thermal conductivity of liquid paraffin-based suspensions in the presence of carbon nano-additives of various sizes and shapes. *Carbon* **2013**, *53*, 277–285. [[CrossRef](#)]
37. He, Q.; Wanga, S.; Liu, Y. Experimental study on thermophysical properties of nanofluids as phase-change material (PCM) in low temperature cool storage. *Energy Convers. Manag.* **2012**, *64*, 199–205. [[CrossRef](#)]
38. Lin, C.-Y.; Wang, J.-C.; Chen, T.-C. Analysis of suspension and heat transfer characteristics of AlO nanofluids prepared through ultrasonic vibration. *Appl. Energy* **2011**, *88*, 4527–4533. [[CrossRef](#)]



© 2018 by the authors. Licensee MDPI, Basel, Switzerland. This article is an open access article distributed under the terms and conditions of the Creative Commons Attribution (CC BY) license (<http://creativecommons.org/licenses/by/4.0/>).